Measurement of surface orientations of transparent objects by use of polarization in highlight

Megumi Saito

Department of Electrical Engineering, Keio University, 3-14-1 Hiyoshi, Kohoku-ku, Yokohama 223-8522, Japan

Yoichi Sato and Katsushi Ikeuchi

Institute of Industrial Science, The University of Tokyo, 7-22-1 Roppongi, Minato-ku, Tokyo 106-8558, Japan

Hiroshi Kashiwagi

Department of Electrical Engineering, Keio University, 3-14-1 Hiyoshi, Kohoku-ku, Yokohama 223-8522, Japan

Received December 23, 1998; accepted April 12, 1999; revised manuscript received May 19, 1999

A method is proposed for obtaining surface orientations of transparent objects by use of polarization in highlight. Since the highlight, the specular component of light reflected from objects, is observed only near the specular direction, it reveals only limited parts of an object's surface. To obtain the orientations of the whole surface of an object, we employ a spherical extended light source. We report the experimental apparatus, a shape recovery algorithm, and a performance evaluation. © 1999 Optical Society of America [S0740-3232(99)02609-5]

OCIS codes: 120.4630, 120.6650, 150.3040, 150.6910, 260.5430, 330.7310.

1. INTRODUCTION

Within the optical community, several noncontact optical methods have been proposed for determining surface orientations. These methods can be separated into two classes: point and surface.[1–4] A point measurement method, which employs optical spots or a beam, scans an entire object surface, measures depth values at each point, and recovers the shape of an object from these measured depth values. A surface measurement method, for example, interferometry or moiré topography, illuminates object surfaces with specially designed light sources, analyzes patterns appearing on the surfaces, and then determines the object shape from this analysis. These methods are effective when applied to a solid surface. Unfortunately, however, no easy methods exist to determine the shapes of transparent objects with incoherent light.

The computer vision community has also developed several methods for determining surface orientations by use of the amount of reflected light (image brightness). Generally speaking, some component of incoming light is immediately reflected from the object surface. This is referred to as surface reflection. Other components penetrate the object surface, are then interreflected among internal pigments of the object, and eventually are emitted into the air. This is referred to as body reflection. There is a massive amount of research, referred to as the shape-from-shading method, to determine surface shape by using body reflection.

Relatively little research has been done to utilize surface reflection for determining the object shape. Ikeuchi[2] employed extended light sources that consisted of a wide planar surface illuminated by three light sources located at three different positions, took three images of specular objects under these extended light sources, and determined surface orientations from image triples at each point by using the photometric stereo method. Nayar *et al.*[3] extended the method by using a spherical diffuser illuminated with many point light sources located around the sphere. Their method determined not only surface orientations but also reflection parameters. Koshikawa[4] measured the polarization of surface reflection components under incoherent light sources and determined surface orientations from the degree of polarization. Wolff and Boult[5,6] also proposed to utilize polarization for determining surface orientation. These methods, although having potential, have not actually been applied to determine surface orientations of transparent surfaces.

Here we propose to use the polarization in surface reflection components for determining shapes of transparent objects. Our method employs the usual incoherent light sources and a CCD camera to determine these shapes. In this paper we describe how we actually set up an experimental apparatus and then evaluate the performance of the method with this apparatus. In Section 2 we review the reflection mechanism. Section 3 describes the algorithm used to determine surface orientations. This section also evaluates the accuracy of the system by

use of simulated images. Section 4 describes the measurement apparatus and its performance. Section 5 concludes the paper.

2. THEORY OF REFLECTION AND POLARIZATION LIGHT

A. Reflection and Highlights

Light reflected from an object consists of several components resulting from surface shapes and object materials. When opaque and inhomogeneous dielectric materials are considered, the following four reflection components, shown in Fig. 1, are significant:

1. A component reflected in the specular direction at the surface with a single bounce: This component is dominant when the wavelength of the incoming light is significantly larger than the microstructure of the surface.
2. A component reflected multiple times along the microstructure.
3. A component that penetrates the surface, interacts with internal pigments, and eventually refracts back out into the air.
4. A component that diffracts from the surface: This component is observed when the microstructure is of the same order as the wavelength of the incident light.

We refer to the first component as the specular component and to the second, third, and fourth components as the diffuse components.[5,7–9] Here the strength of the fourth component is much smaller than that of the other components and usually can be ignored, except when the microstructure has the repeated pattern in which the cycle length is the same as the wavelength of the incoming light. When the surface is perfectly smooth, we can obtain the first and the third components. Light reflected from typical surfaces consists of all four components.

The third component is repeatedly reflected, refracted, and absorbed by material elements such as pigments, and its color (spectral powder distribution) is intrinsic to the object. On the other hand, the first and the second components have the same color as the incident light. The first component returns a large amount of energy to the particular emitting direction (specular direction). The second component has less energy than the first component. We refer to the sum of the first and the second components as the highlight. In particular, the surface of transparent objects reveals only the highlight.

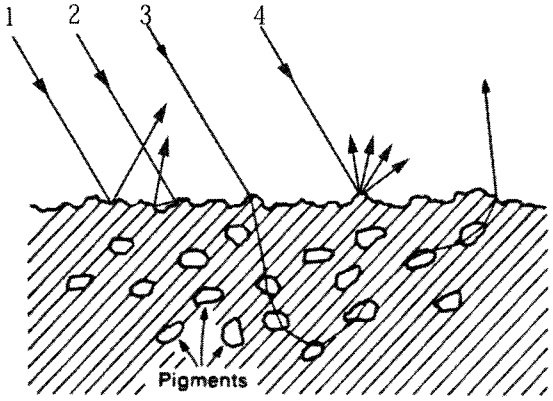

Fig. 1. Mechanism of reflection.

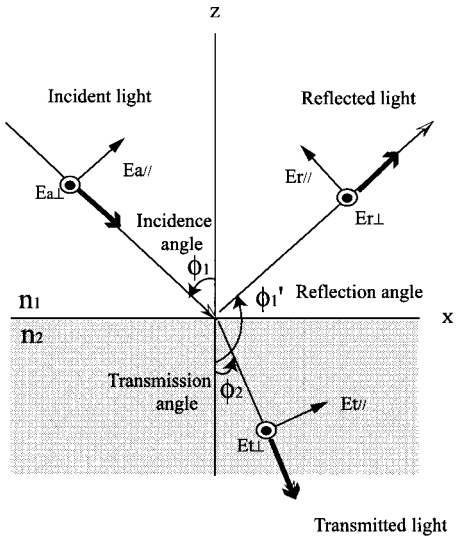

Fig. 2. Fresnel reflection.

B. Fresnel Reflection Formula

(The Fresnel reflection formula is discussed in detail in Ref. 10.) Let us assume that an interface surface between media 1 and 2 is located in the $x-y$ plane as shown in Fig. 2. The refractive indices of media 1 and 2 are n_1 and n_2, respectively. The light wave in the $x-z$ plane strikes the interface surface: One part of the light is reflected at the origin; the other part is refracted and transmitted into medium 2. Here we assume that the object consists of transparent dielectric materials so that the absorption can be ignored when visible light is considered.

The polarization components of incident, reflected, and transmitted light parallel or perpendicular to the $x-z$ plane are expressed by the subscript $\parallel$ or $\perp$, respectively. We define incidence angle ϕ_1, reflection angle ϕ_1', and transmission angle ϕ_2 as depicted in Fig. 2. Incident and reflected light go through the same medium. As a result of this, we get $\phi_1 = \pi - \phi_1'$. The incident, reflected, and transmitted components of the electric field vector parallel to the $x-z$ plane, $E_{a\parallel}$, $E_{r\parallel}$, and $E_{t\parallel}$, are

$$E_{a\parallel} = A_\parallel \exp\{i[\omega t - k_1(x \sin\phi_1 + z \cos\phi_1)]\},$$

$$E_{r\parallel} = R_\parallel \exp\{i[\omega t - k_1(x \sin\phi_1 - z \cos\phi_1)]\},$$

$$E_{t\parallel} = T_\parallel \exp\{i[\omega t - k_2(x \sin\phi_2 + z \cos\phi_2)]\}, \quad (1)$$

where $A_\parallel$, $R_\parallel$, and $T_\parallel$ represent the amplitudes of the three components, ω represents the angular frequency, and k_1 and k_2 represent the wave number, where the wave number is expressed as $2\pi/\lambda$; λ is the wavelength. The subscripts a, r, and t denote incident, reflected, and transmitted light, respectively. The perpendicular component is expressed in a similar manner. The relation between the incidence angle ϕ_1 and the transmission angle ϕ_2 of the refracted light when it is penetrating from one medium to another is given by Snell's law:

$$n_1 \sin\phi_1 = n_2 \sin\phi_2. \quad (2)$$

The boundary condition of the Maxwell equation requires that components of electric and magnetic fields on the boundary plane must be continuous at the plane. Thus, the amplitude of the transmitted light in medium 2 must be equivalent to the sum of the amplitude of the incident light and one of the reflected lights in medium 1 in the x and the y directions. From this we obtain

$$E_{aj} + E_{rj} = E_{tj}, \qquad H_{aj} + H_{rj} = H_{tj} \qquad (j = x, y), \tag{3}$$

where E and H denote the electric and the magnetic fields, respectively. Equations (3) can be combined with Eqs. (1) and (2) to yield the Fresnel formula that expresses the reflectance of light amplitude with respect to the parallel and the perpendicular components, $r_{\parallel}$ and $r_{\perp}$:

$$r_{\parallel} = \frac{E_{r\parallel}}{E_{a\parallel}} = \frac{\tan(\phi_1 - \phi_2)}{\tan(\phi_1 + \phi_2)},$$

$$r_{\perp} = \frac{E_{r\perp}}{E_{a\perp}} = -\frac{\sin(\phi_1 - \phi_2)}{\sin(\phi_1 + \phi_2)}. \tag{4}$$

The image intensity I is expressed as

$$I = nE^2/2\sqrt{\mu_0}, \tag{5}$$

where n stands for a refractive index of each medium and μ_0 is permeability in vacuum. Likewise, from Eqs. (4), the reflectance of the light intensity is given by

$$F_{\parallel} = \frac{\tan^2(\phi_1 - \phi_2)}{\tan^2(\phi_1 + \phi_2)},$$

$$F_{\perp} = \frac{\sin^2(\phi_1 - \phi_2)}{\sin^2(\phi_1 + \phi_2)}. \tag{6}$$

The intensity reflectances $F_{\parallel}$ and $F_{\perp}$ are referred to as the Fresnel reflection coefficients. Equations (6) indicate that there is an angle of incidence that yields $F_{\parallel} = 0$. This angle of incidence is referred to as the Brewster angle ϕ_b. The Brewster angle is given by $\phi_1 + \phi_2 = \pi/2$ and Snell's law as

$$\phi_b = \arctan(n_2/n_1). \tag{7}$$

3. MEASUREMENT OF SURFACE ORIENTATIONS OF TRANSPARENT OBJECTS

A. Theory of Measurement

Usually natural light is unpolarized; it oscillates randomly in all directions. Sometimes such natural light becomes polarized, for example, when transmitted through a birefringent crystal or when reflected from an object surface. When part of the light is polarized, that portion is called partially polarized light. Here we study reflection from objects. Reflected light is the sum of the diffuse and the specular components. The diffuse component of reflected light is typically unpolarized; however, it can be ignored in transparent objects.

We determine the surface normal from the direction of polarization in the specular component. When light waves, transverse electromagnetic waves, propagate along one direction, the electric field vector lies approximately on a plane perpendicular to the transverse line. The electromagnetic wave oscillates on the plane, and these oscillations may be biased, or polarized, in a certain direction. This polarization depends on the incidence angle and the orientation of the plane of incidence.

The geometry of our measurement system is shown in Fig. 3. We define the plane of incidence as the one that includes the direction of a light source, a viewer, and a surface normal. In transparent objects the diffuse reflection component can be ignored, and absorption does not occur. The reflection angle is equal to the incidence angle. We can obtain surface-normal orientations by using the orientation of the plane of incidence and the reflection angle at each point of the object's surface. The orientation of the plane is denoted θ, measured around the viewer's line of sight, and the angle of incidence is denoted ϕ, measured on the plane of incidence.

As is seen from Eqs. (6), the intensity reflectance depends on the direction of the plane of oscillation, parallel or perpendicular. The measured brightness changes when a polarizer is rotated in front of a detector. We define the maximum and the minimum of the light intensity as $I_{\max}$ and $I_{\min}$, respectively. The sum of $I_{\max}$ and $I_{\min}$ is equal to the total light intensity of the specular component, I_s.

$$I_{\max} = \frac{F_{\perp}}{F_{\parallel} + F_{\perp}} I_s, \qquad I_{\min} = \frac{F_{\parallel}}{F_{\parallel} + F_{\perp}} I_s. \tag{8}$$

Since $I_{\min}$ is the component parallel to the plane of incidence, the orientation of the plane of incidence θ can be determined when $I_{\min}$ appears while the polarizer is rotated.

We define the degree of polarization, ρ, as

$$\rho = \frac{I_{\max} - I_{\min}}{I_{\max} + I_{\min}}. \tag{9}$$

The degree of polarization is 0 for unpolarized light and 1 for linearly polarized light. When the incidence angle is equal to the Brewster angle, only the perpendicular component appears in the reflected light; the reflected light is linearly polarized, and the degree of polarization is 1.

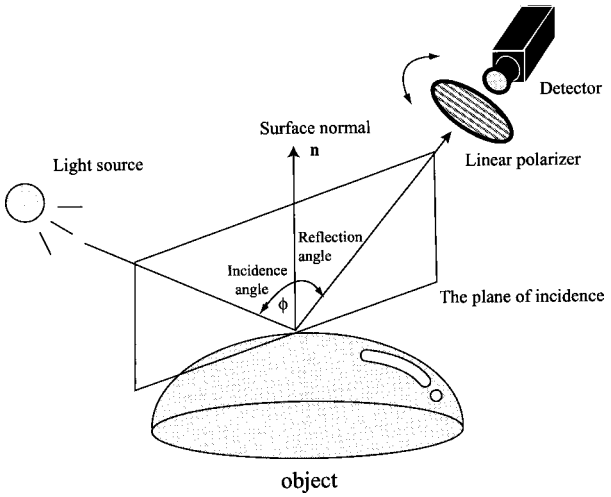

Fig. 3. Surface normal of object.

Substituting Eqs. (6) and (8) for Eq. (9), consider Snell's law; the degree of polarization ρ is given by

$$\rho = \frac{2 \sin \phi \tan \phi (n^2 - \sin^2 \phi)^{1/2}}{n^2 - \sin^2 \phi + \sin^2 \phi \tan^2 \phi}. \tag{10}$$

The degree of polarization ρ is a function of the angle of incidence ϕ under a given refractive index n. Thus, from the measured degree of polarization, we can obtain the angle of incidence ϕ from Eq. (10).

We can summarize the measurement algorithm as follows:

1. While rotating the polarizer, we measure the light intensity to find I_{max} and I_{min} at each pixel.
2. From Eq. (9), the component parallel to the plane of incidence is I_{min}. Thus, by finding the polarizer rotation angle that provides the minimum intensity, we can obtain the angle of the plane, θ.
3. The degree of polarization is given by Eq. (8) with the measured I_{max} and I_{min}.
4. Equation (10) provides the degree of polarization from the refractive index n and the incidence angle ϕ. By inversely solving the equation from a given refractive index and measuring the degree of polarization, we can obtain the incidence angle.

B. Evaluation of Accuracy

This section evaluates the accuracy of the system. We measure the deviation of the orientation of the plane of incidence and the angle of incidence depending on errors in measured light intensity.

First we fix the refractive index n. We also choose the angle of incidence ϕ and the orientation of the incidence plane, θ. From these two values we can obtain the maximum, I_{max}, and the minimum, I_{min}, of the light intensity. Then Gaussian noise is added to I_{max} and I_{min}. The angle of incidence ϕ and the orientation of the incidence plane, θ, are inversely calculated by use of these two values and the difference between the real and the estimated values of the incident angle and the orientation of the incidence plane. This process is repeated 1000 times to yield the standard deviations of these two angles.

Figures 4(a) and 4(b) show the dependence of the standard deviation of θ and ϕ on the error rate of intensity. Here, the refractive index is fixed at 1.5. The change in the standard deviation as a function of the angle of incidence appears in Fig. 4(c). The error rate of intensity is fixed at 10%.

From this evaluation we can conclude that the error in the incidence orientation is 2.2° and that that of the angle of incidence is 1.1° for a 15% error range in the intensity measurement. The error in θ and ϕ is linearly proportional to the error in intensity, and thus we can control the error range in θ and ϕ by maintaining a lower error in intensity. In particular, since the intensity error is affected by sampling with eight-bit resolution, we can reduce the intensity error by illuminating objects brightly enough to make intensity values larger. As is shown in Fig. 4(c), when the intensity error rate is fixed at 10%, its standard deviation has a maximum of ~3.1°, at 60°. Since the Brewster angle is 56.3°, the measurement system is most affected by noise in the vicinity of the Brewster angle.

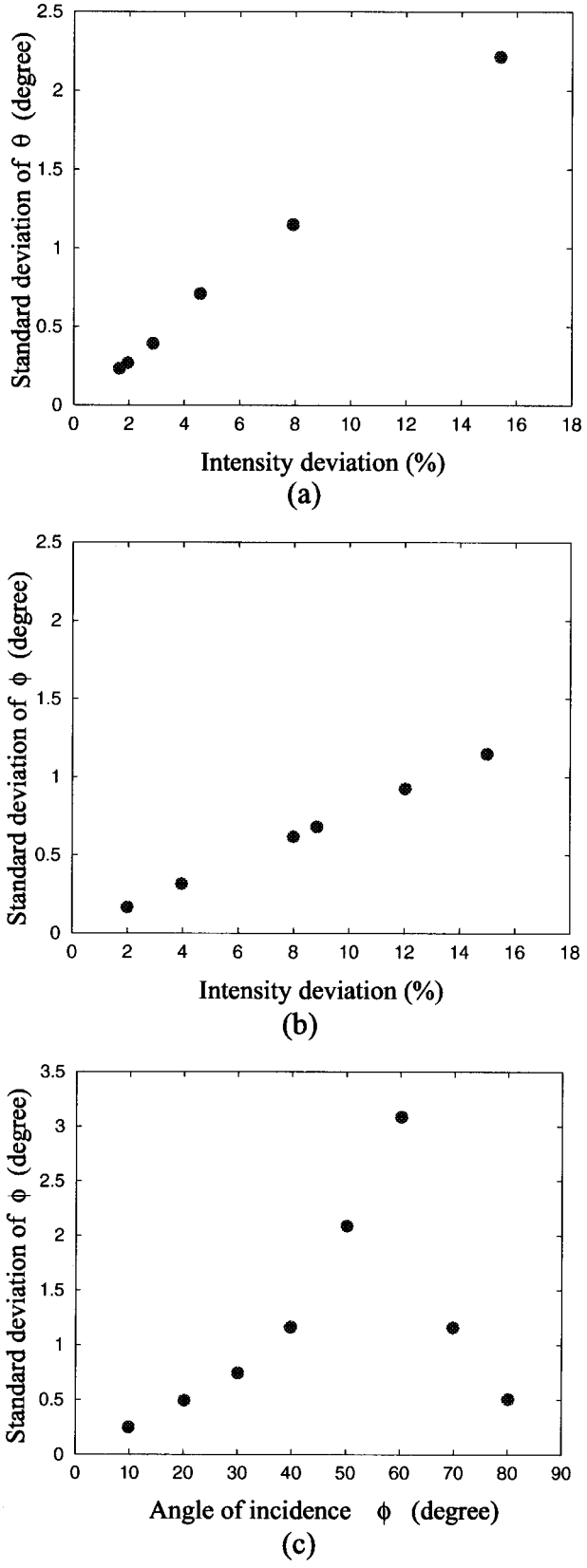

Fig. 4. Simulation result.

C. Experimental Method

We conducted an experiment on measuring a transparent object shape. The setup is shown in Fig. 5. A white 150-W incandescent electric lamp was used as the light source. As an object for measuring, we employed a 30 mm × 30 mm × 3 mm plane glass plate, which consisted of soda lime glass whose refractive index was 1.523. We used a rotary stage to position the object in an arbitrary direction. A monochromatic CCD camera was used as a reflected light detector. The image of the CCD had 480 × 512 pixels, and each pixel had 8 bits, that is, 256 gradations.

The approach employed in this experiment was as follows. We repeatedly took images with the CCD sequentially as we rotated the polarizer in front of the camera at an angle from 0° through 180° at intervals of 5°. The result was that we obtained 36 images. A variance in the intensity of the light at each pixel could be observed in the images. By using the variations, we were able to obtain the maximum and the minimum intensity. Since a 5° interval for sampling a polarized angle may not be so small, a discrepancy between experimental data and the actual values of the maximum and the minimum may have occurred. To avoid this problem, we fitted a sinusoid function to the experimental data by using the nonlinear root mean square method and estimated the actual maximum and minimum values.

As is described in Subsection 3.A, surface normal orientations can be calculated from $I_{\max}$ and $I_{\min}$. We conducted an experiment by rotating the object at a reflection angle from 10° to 80° at intervals of 10°. The orientation of the plane of incidence was fixed at 90° as shown in Fig. 5. We employed an algorithm, using the reflection theory, and calculated surface orientations based on experimental data at each pixel. Here it can be presumed that the lens used in this experiment had a focal length long enough that its projection geometry can be approximated as the orthographic projection. It is appropriate that all results at each pixel were equivalent, because the object had a plane surface. Therefore we calculated the average and the standard deviation of both the orientations of the plane of incidence and the angles of incidence obtained at all pixels. The average is used as the result of this experiment.

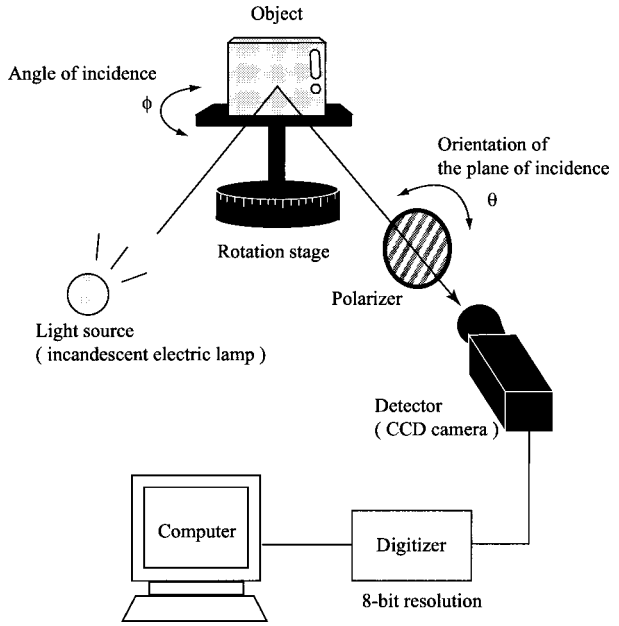

Fig. 5. Experimental setup.

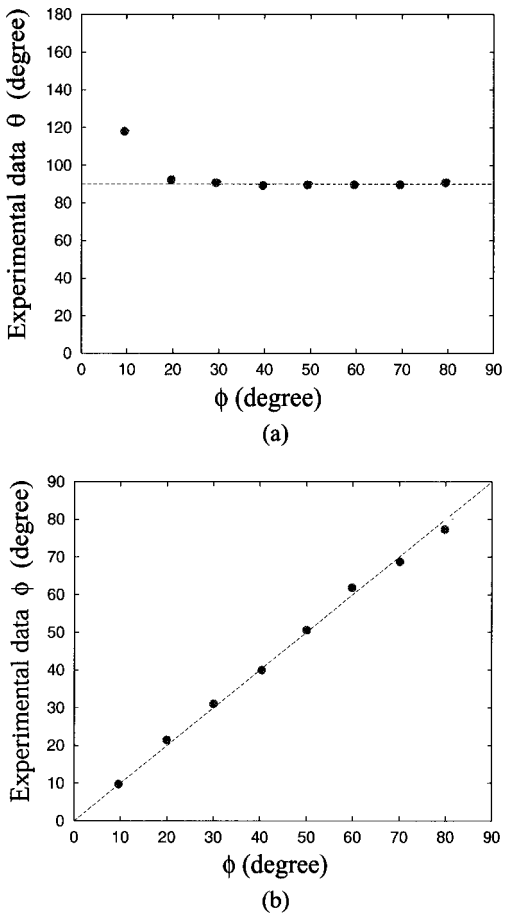

Fig. 6. Experimental results: (a) orientation of the plane of incidence; (b) angle of incidence.

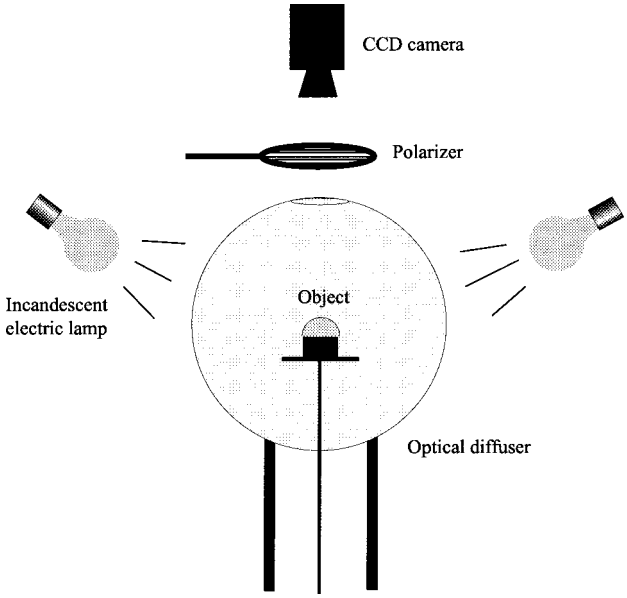

Fig. 7. Experimental setup.

D. Experimental Results

The results of the orientation of the incident plane, θ, and the angle of incidence, ϕ, obtained experimentally are depicted as a function of ϕ in Figs. 6(a) and 6(b), respectively. In Fig. 6(a) the calculated orientations of the incident plane are close to the real values, 90°, depicted by the dotted line, except near 10° incidence; in Fig. 6(b) the calculated incidence angles are close to the real data. At small incidence angles the degree of polarization is also small, and the amplitude of the sinusoidal function is relatively smaller than other areas; fitting errors of the nonlinear minimization become larger. We can, however, improve this by increasing the brightness of the images, thereby resulting in a larger amplitude of the function.

4. MEASUREMENT WITH A SPHERICAL EXTENDED LIGHT SOURCE

A. Theory of Measurement

The previous section evaluated the accuracy of the proposed algorithm and demonstrated its effectiveness. In this section we propose a practical measurement system that employs an extended light source. As stated previously, however, the highlight is observed only near the specular direction; thus, if we use an ordinal point light source, we can obtain surface orientations only at relatively limited areas that satisfy the specular geometry. To overcome this problem, we employ a spherical extended light source.

An extended light source emits light from a region with

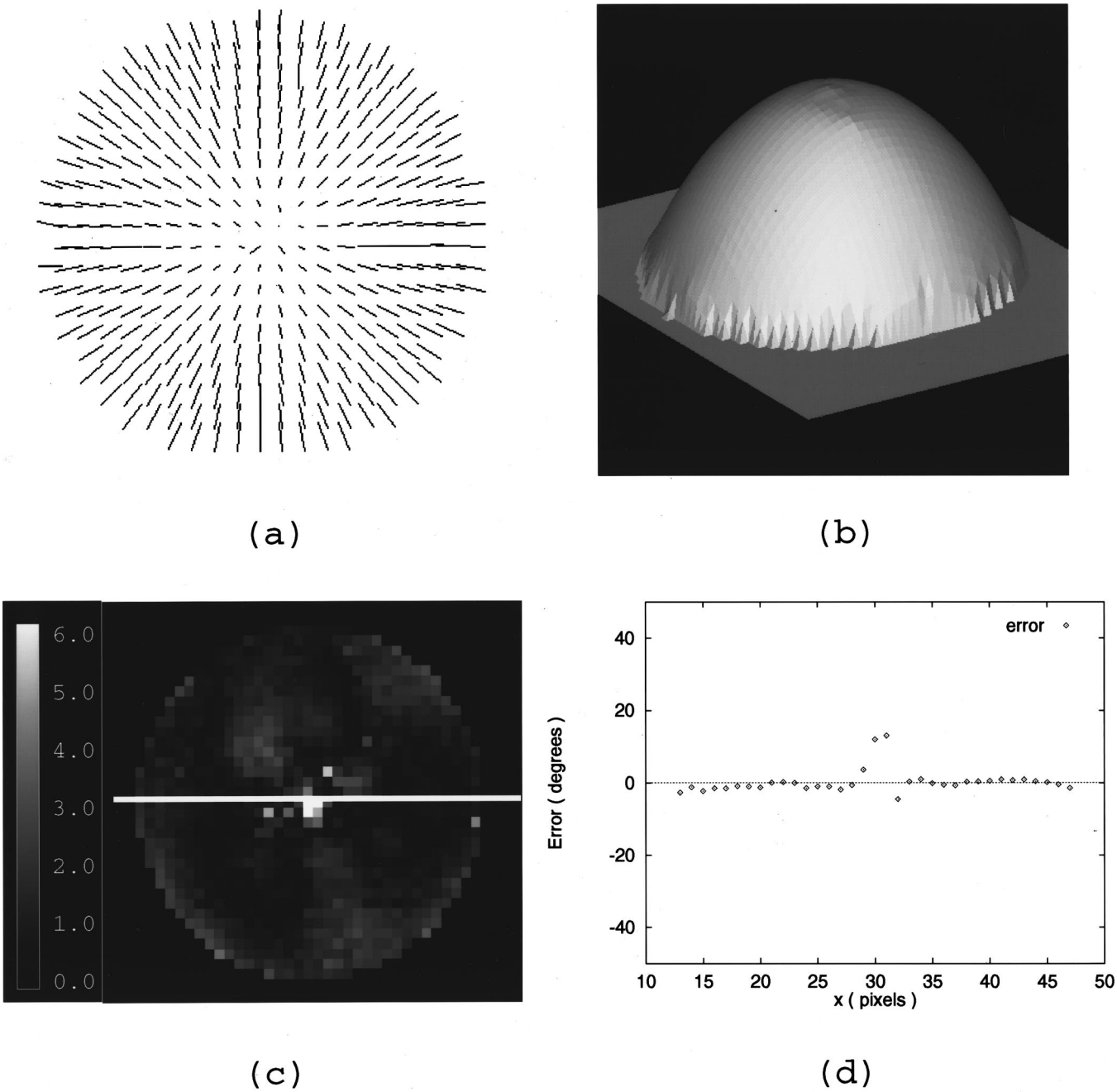

Fig. 8. Result of measurement of the object shape.

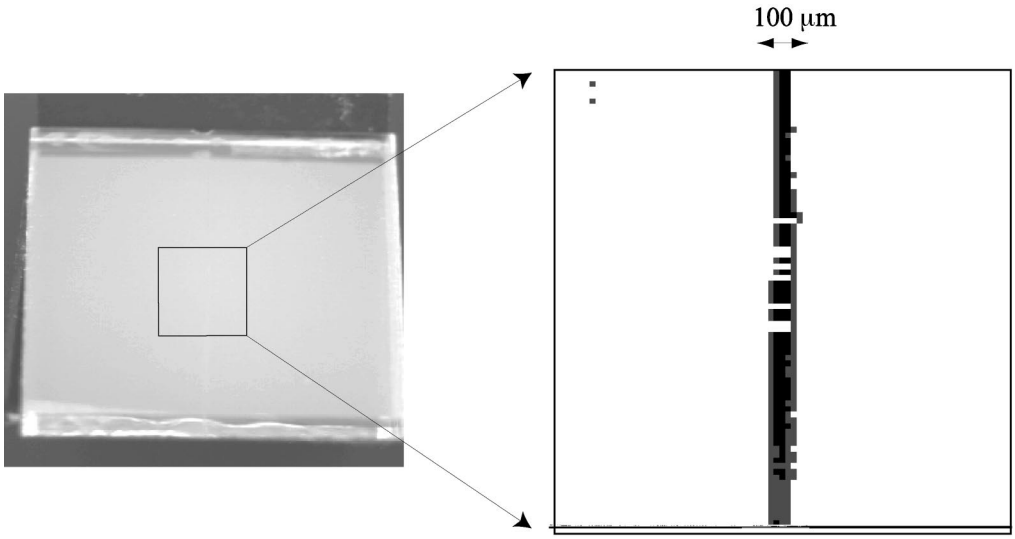

Fig. 9. Result of flaw inspection.

some area. This is in contrast to a point light source, such as an electric lamp, that emits a spherical light wave from one point, with a neglible area, to surrounding directions. The highlight depends on the direction of the light source and viewing direction, but it becomes possible to reduce the dependence on the direction of the light source by using an extended light source. In particular, a spherical extended light source, where the object is placed at the center of the sphere, can project light to the object from all directions. The highlight can be generated over the entire surface of the object. It becomes possible to obtain the orientations of the entire surface without scanning the camera.

The experimental apparatus with the spherical extended light source is depicted in Fig. 7. The spherical-extended light source is an optical diffuser, a white translucent plastic sphere whose diameter is 40 cm; the sphere is illuminated with three incandescent electric lamps placed at intervals of 120°. An object is placed in the center of this sphere. Images of the object are taken by a CCD camera through a hole located at the north pole of the sphere.

B. Experimental Results

We conducted an experiment on measuring an object, a plastic hollow hemisphere with a refractive index of 1.55 and a diameter of 6 cm. In the same way described in Section 3, we repeatedly took images sequentially as we rotated the polarizer in front of the CCD camera. Figure 8(a) depicts the obtained surface normals as needles, displayed at every 20 pixels. From the figure, the directions of the needles are rotationally symmetrical with respect to the center of the object, and their lengths increase along the radius direction of the object. We concluded that the obtained surface normalizations are consistent with those of the object. For visualization, Fig. 8(b) shows the object shape calculated from the obtained surface normals.

Figure 8(c) visually depicts the difference between the estimated angle of incidence and the real angle of incidence. In this figure a brighter pixel represents a larger error. The region in which the angle of incidence is more than 50° is excluded in Fig. 8(c), since the region is too close to the occluding boundary of the hemisphere.

Figure 8(d) shows the plot of the error in the angle of incidence along the scan line drawn in Fig. 8(c). From these results we can see that the error becomes significantly large at small angles of incidence, whereas the error is small otherwise. This is because the spherical extended light source used in our experiments has a hole through which the camera sees the object. Because of this hole, the light source does not cover the region of small angle of incidence. The average error in the angle of incidence was 0.82° in this experiment.

For the next experiment we demonstrated the ability of the system to detect flaws on the surfaces of transparent objects. We created a flaw whose width was ~100 μm on the glass plate used in Section 3, and we measured surface normals by the same procedure. Figure 9 shows this result. The black region in the resulting image represents pixels with normals that deviate from the average orientation.

5. CONCLUSION

This paper proposed a method for measuring surface orientations of transparent objects by use of polarization in highlight. The paper also demonstrated the method's effectiveness and evaluated its accuracy by describing experiments performed with synthesized and real images. We also proposed employing a spherical extended light source for the system because the highlight, the specular reflection of light from objects, is observed only near the specular direction and appears on relatively limited parts of an object's surface if an ordinal point light source is used. The experimental results show that the obtained surface orientations are highly accurate and that the proposed method is effective. We also demonstrated the ability of the system to detect flaws on the surfaces of transparent objects and the potential for practical shape-inspection applications of the system.

M. Saito may be reached at megumi@cvl.iis.u-tokyo.ac.jp.

REFERENCES

1. T. Tanitagai, *Applied Optics: Guide of Optical Measurement* (Maruzen, Tokyo, 1988).
2. K. Ikeuchi, "Determining surface orientations of specular surfaces by using the the photometric stereo method," IEEE Trans. Pattern. Anal. Mach. Intell. **3**, 661–669 (1981).
3. S. K. Nayar, K. Ikeuchi, and T. Kanade, "Determining shape and reflectance of hybrid surface by photometric sampling," IEEE Trans. Rob. Autom. **6**, 418–431 (1990).
4. K. Koshikawa, "A polarimetric approach to shape understanding of glossy objects," in *Proceedings of International Joint Conference on Artificial Intelligence* (Morgan Kaufmann, San Mateo, Calif., 1979), pp. 493–495.
5. L. B. Wolff and T. E. Boult, "Constraining object features using a polarization reflectance model," IEEE Trans. Pattern. Anal. Mach. Intell. **13**, 167–189 (1991).
6. L. B. Wolff, "Spectral and polarization stereo methods using a single light source," in *Proceedings of International Conference on Computer Vision* (Institute of Electrical and Electronics Engineers, New York, 1987), pp. 708–715.
7. K. E. Torrance and E. M. Sparrow, "Theory for off-specular reflection from roughened surfaces," J. Opt. Soc. Am. **57**, 1105–1114 (1967).
8. S. K. Nayar, K. Ikeuchi, and T. Kanade, "Surface reflection: physical and geometrical perspectives," IEEE Trans. Pattern. Anal. Mach. Intell. **13**, 611–634 (1991).
9. S. Shafer, "Using color to separate reflection components," Color Res. Appl. **10**, 210–218 (1985).
10. M. Ohtsu, *Modern Optical Science* (Asakura, Tokyo, 1994).